Dietary and genetic evidence for phosphate toxicity accelerating mammalian aging

Mutsuko Ohnishi* and M. Shawkat Razzaque*,†,[1]

*Department of Oral Medicine, Infection, and Immunity, Harvard School of Dental Medicine, Boston, Massachusetts, USA; and †Department of Pathology, Nagasaki University Graduate School of Biomedical Sciences, Nagasaki, Japan

ABSTRACT **Identifying factors that accelerate the aging process can provide important therapeutic targets for slowing down this process. Misregulation of phosphate homeostasis has been noted in various skeletal, cardiac, and renal diseases, but the exact role of phosphate toxicity in mammalian aging is not clearly defined. Phosphate is widely distributed in the body and is involved in cell signaling, energy metabolism, nucleic acid synthesis, and the maintenance of acid-base balance by urinary buffering. In this study, we used an *in vivo* genetic approach to determine the role of phosphate toxicity in mammalian aging. Klotho-knockout mice (*klotho*$^{-/-}$) have a short life span and show numerous physical, biochemical, and morphological features consistent with premature aging, including kyphosis, uncoordinated movement, hypogonadism, infertility, severe skeletal muscle wasting, emphysema, and osteopenia, as well as generalized atrophy of the skin, intestine, thymus, and spleen. Molecular and biochemical analyses suggest that increased renal activity of sodium-phosphate cotransporters (NaPi2a) leads to severe hyperphosphatemia in *klotho*$^{-/-}$ mice. Genetically reducing serum phosphate levels in *klotho*$^{-/-}$ mice by generating a *NaPi2a* and *klotho* double-knockout (*NaPi2a*$^{-/-}$/*klotho*$^{-/-}$) strain resulted in amelioration of premature aging-like features. The *NaPi2a*$^{-/-}$/*klotho*$^{-/-}$ double-knockout mice regained reproductive ability, recovered their body weight, reduced their organ atrophy, and suppressed ectopic calcifications, with the resulting effect being prolonged survival. More important, when hyperphosphatemia was induced in *NaPi2a*$^{-/-}$/*klotho*$^{-/-}$ mice by feeding with a high-phosphate diet, premature aging-like features reappeared, clearly suggesting that phosphate toxicity is the main cause of premature aging in *klotho*$^{-/-}$ mice. The results of our dietary and genetic manipulation studies provide *in vivo* evidence for phosphate toxicity accelerating the aging process and suggest a novel role for phosphate in mammalian aging.—Ohnishi, M., Razzaque, M. S. Dietary and genetic evidence for phosphate toxicity accelerating mammalian aging. *FASEB J.* 24, 3562–3571 (2010). www.fasebj.org**

Key Words: klotho · *NaPi2a* · *survival* · *fertility* · *emphysema* · *calcification*

AGING IS A COMPLEX BIOLOGICAL process controlled and influenced by numerous genetic, humoral, and environmental factors (1–3). For instance, DNA damage through oxidative stress, among others, is thought to be an important contributing factor in aging and has been extensively studied in mammalian systems (4–11). Recent *in vivo* studies, however, have identified additional factors that can significantly affect the overall deterioration of physiological functions for various organ systems and thus accelerate mammalian aging. Phosphorus is a widely distributed mineral ion in the body that is an essential component of cell signaling, energy metabolism, and nucleic acid synthesis (12). In this study, we examined the effects of phosphate toxicity in mammalian aging. We used hyperphosphatemic *klotho*-knockout mice as an *in vivo* model to determine the effects of phosphate toxicity on mammalian aging.

Systemic regulation of phosphate homeostasis is a complex process, usually maintained by a delicate coordination between the intestine and the kidney (13–15). After intestinal absorption, circulating phosphorus is taken up by cells that need it, accumulates in the bone matrix protein, and enters the kidney. About 95% of filtered phosphate is reabsorbed in the proximal tubules of the kidneys. Phosphate from the proximal tubular lumen moves across tubular epithelial cells and effluxes at the basolateral membrane to enter blood vessels. The identification of specific phosphate transporters in the intestine and kidney has enhanced our understanding of phosphate metabolism. Sodium-phosphate (NaPi) cotransporters that are located in the intestine and the kidney play an important role in maintaining physiological phosphate balance (16). NaPi2b in the intestine aids in phosphate absorption, while the NaPi2a and NaPi2c transporters, in a sodium-dependent manner, assist in reabsorption of filtered phosphate in the kidney according to the needs of the body. The *klotho*-knockout mice develop severe hyperphosphatemia by 3 wk of age and remain hyperphos-

[1] Correspondence: Department of Medicine, Infection and Immunity, Harvard School of Dental Medicine, Research and Education Bldg., Rm. 304, 190 Longwood Ave., Boston, MA 02115, USA. E-mail: mrazzaque@hms.harvard.edu

doi: 10.1096/fj.09-152488

0892-6638/10/0024-3562 © FASEB

phatemic throughout their life span due to increased renal activity of the NaPi system (17–19).

Genetic inactivation of *klotho* in mice results in a phenotype resembling human aging, including kyphosis, muscle wasting, infertility, atherosclerosis, ectopic calcifications, generalized tissue atrophy, and an extremely shortened life span (20, 21). To determine whether phosphate toxicity can accelerate the aging-like features in *klotho*-knockout mice, we genetically reduced serum phosphate levels in *klotho*-knockout mice by generating *NaPi2a*; *klotho* double-knockout ($NaPi2a^{-/-}/klotho^{-/-}$; DKO) mice. Our results suggest that phosphate toxicity accelerates the mammalian aging process and that reducing the phosphate burden can delay the aging.

MATERIALS AND METHODS

Generation of $NaPi2a^{-/-}/klotho^{-/-}$ mice

We interbred heterozygous *klotho* mutants (Lexicon Genetics; Mutant Mouse Regional Resource Centers, University of California, Davis, CA, USA) with heterozygous *NaPi2a* mutants to obtain compound heterozygous animals, which were then interbred to generate the desired double-homozygous mutants ($NaPi2a^{-/-}/klotho^{-/-}$; refs. 22, 23). Routine PCR was used to genotype the mice as detailed earlier (24). All studies performed were approved by the Harvard Medical School Institutional Animal Care and Use Committee (Boston, MA, USA).

Animal feeding

Wild-type, $klotho^{-/-}$, and $klotho^{-/-}/NaPi2a^{-/-}$ double-mutant mice were housed in a barrier facility and maintained under specific pathogen-free conditions during the entire study period. After weaning, at 3 wk of age, mice were divided into 2 groups: wild-type, $klotho^{-/-}$, and $klotho^{-/-}/NaPi2a^{-/-}$ mice continued to receive a normal phosphate diet (NPD: 0.6%) *ad libitum*, while an experimental group of $klotho^{-/-}/NaPi2a^{-/-}$ mice received a high-phosphate diet (HPD: 1.2%) from 3 wk onwards for the rest of their lives. Mice were provided with food purchased from LabDiet/TestDiet (St. Louis, MO, USA). The energy in the NPD (kcal/g) was provided by protein at 23.1%, with fat and carbohydrate contributing 21.6 and 55.1%, respectively. The energy distribution in the HPD (kcal/g) was very similar, with protein providing 23.2%, fat supplying 22.1%, and carbohydrate contributing 54.7%.

Gross phenotype and body weight

The total body weight of wild-type, $klotho^{-/-}$, and $NaPi2a^{-/-}/klotho^{-/-}$ mice fed with either NPD or HPD was measured every week, starting at 3 wk of age until 20 wk of age. The maximum survival of $klotho^{-/-}$ mice and $NaPi2a^{-/-}/klotho^{-/-}$ mice fed with HPD was ~15 wk.

Measurement of serum phosphate and calcium

Blood was obtained by cheek pouch bleeding of wild-type, $klotho^{-/-}$, and $NaPi2a^{-/-}/klotho^{-/-}$ mice fed with either NPD or HPD. Serum was isolated by centrifugation at 3000 *g* for 10 min and stored at −80°C. Serum phosphorus and calcium were determined by colorimetric measurements using the Stanbio Phosphorus Liqui-UV Test and Calcium (Arsenazo) LiquiColor Test, respectively (Stanbio Laboratory, Boerne, TX, USA).

Measurement of serum creatinine and 1,25-dehydroxyvitamin D

Serum creatinine levels were determined using the Stanbio creatinine kits (Stanbio Laboratory), as recommended by the manufacturer. The levels of 1,25-dehydroxyvitamin D were measured in serum obtained from wild-type, $klotho^{-/-}$, and $NaPi2a^{-/-}/klotho^{-/-}$ mice fed with either NPD or HPD using a kit purchased from IDS (Fountain Hills, AZ, USA).

Histological analyses

Soft tissues obtained from wild-type, $klotho^{-/-}$, and $NaPi2a^{-/-}/klotho^{-/-}$ mice fed with either NPD or HPD at 9–12 wk were fixed with 4% paraformaldehyde and 10% buffered formalin or Carnoy's solution and were subsequently embedded in paraffin. Four- to 6-μm paraffin sections of various tissues were mounted on SuperFrost Plus glass slides. Sections were then stained with hematoxylin and eosin and von Kossa. Histological samples were observed by light microscopy (25, 26).

Calcification analyses

To determine the effects of hyperphosphatemia on ectopic calcification, sections were prepared from heart, lung, and kidney of wild-type, $klotho^{-/-}$, and $NaPi2a^{-/-}/klotho^{-/-}$ mice fed with either NPD or HPD and were stained with von Kossa to visualize mineralized tissues by light microscopy. The von Kossa staining procedure is detailed in an earlier publication (27).

Immunohistochemical staining

Immunostaining was performed as described previously (26, 28). Briefly, kidneys obtained from wild-type and $klotho^{-/-}$ mice were fixed in 10% formalin and embedded in paraffin. Paraffin sections were deparaffinized and incubated in blocking solution for 30 min and then incubated overnight with polyclonal anti-NaPi2a antibody (dilution 1:100) at 4°C. Slides were washed with PBS and incubated with secondary antibody (dilution, 1:100) for 30 min. After a PBS wash, coverslips were placed on slides using mounting medium. The expression of NaPi2a was visualized using a bright-field microscope. Rabbit serum in place of primary antibody was used as a negative control. Kidney sections prepared from $NaPi2a^{-/-}$ mice and incubated with NaPi2a antibody did not show any staining.

TUNEL staining

The extent of apoptosis in wild-type, $klotho^{-/-}$, and $NaPi2a^{-/-}/klotho^{-/-}$ mice fed with either NPD or HPD was determined by TUNEL assays using a commercial kit (Roche Diagnostics, Indianapolis, IN, USA) according to the manufacturer's instructions (29, 30). Briefly, deparaffinized sections of various soft tissues, including lung, muscle, and kidney, were treated with Proteinase K for 15–30 min at 37°C. After the slides were rinsed with PBS, they were treated with the TUNEL reaction mixture for 60 min at 37°C in a humidified chamber. Slides were washed with PBS and incubated for another 30 min with peroxidase solution. TUNEL-positive cells were visualized following incubation of the sections in the diaminobenzidine substrate. As a negative control, the

TUNEL reaction mixture was substituted by a control solution provided in the kit. The numbers of TUNEL-positive cells were randomly counted for at least 5 fields per millimeter squared area of different tissues.

Statistical analysis

Statistically significant differences between groups were evaluated either by the Student's *t* test or the Mann-Whitney *U* test for a comparison between 2 groups. All values are expressed as means ± SE. A value of $P < 0.05$ was considered to be statistically significant. All analyses were performed using Microsoft Excel (Microsoft, Redmond, WA, USA).

RESULTS

NaPi2a and phosphate toxicity in *klotho*$^{-/-}$ mice

Compared with wild-type mice, *klotho*$^{-/-}$ mice showed increased expression of NaP_i2a protein in the luminal side of the proximal tubules by immunohistochemistry (Supplemental Fig. 1). Increased expression of NaP_i2a was associated with markedly increased serum phosphate levels in *klotho*$^{-/-}$ mice. To determine the pathological consequences of phosphate toxicity for mammalian aging, we genetically reduced serum phosphate levels in *klotho*$^{-/-}$ mice by generating *NaPi2a*$^{-/-}$/*klotho*$^{-/-}$ double mutants.

Induction of phosphate toxicity in *NaPi2a*$^{-/-}$/*klotho*$^{-/-}$ mice

To determine whether phosphate toxicity in *klotho*$^{-/-}$ mice accelerates aging-like phenotypes, we generated a new mouse model with reduced serum phosphate levels by interbreeding *NaPi2a* and *klotho* mutants. Consistent with our earlier observations, the *NaPi2a*$^{-/-}$/*klotho*$^{-/-}$ double mutants were viable and larger in size than the *klotho*$^{-/-}$ mice (**Fig. 1**). At birth, *NaPi2a*$^{-/-}$/*klotho*$^{-/-}$-*mutant* mice were indistinguishable from their littermates. At 3 wk of age, *NaPi2a*$^{-/-}$/*klotho*$^{-/-}$ double mutants (12.4±0.2 g) were smaller than wild type (16±0.4 g) but larger in size to *klotho*$^{-/-}$ mice (10.4±0.3 g; Fig. 1).

At 6–9 wk of age, *NaPi2a*$^{-/-}$/*klotho*$^{-/-}$ double-mutant mice fed with NPD were still smaller than their wild-type littermates (*NaPi2a*$^{-/-}$/*klotho*$^{-/-}$: 19.9±0.5 g *vs.* wild type: 28.8±1.4 g at 9 wk) and larger in size than the *klotho*$^{-/-}$ mice (*klotho*$^{-/-}$: 11.3±0.4 g at 9 wk). However, at 9 wk the average body weight of *NaPi2a*$^{-/-}$/*klotho*$^{-/-}$ double mutants fed with HPD was 11.7 ± 0.6 g (Fig. 1).

Estimation of phosphate toxicity in *NaPi2a*$^{-/-}$/*klotho*$^{-/-}$ mice

Serum phosphate and calcium levels were measured in 3-, 6- and 9-wk-old wild-type, *klotho*$^{-/-}$, and *NaPi2a*$^{-/-}$/*klotho*$^{-/-}$mice fed with either NPD or HPD. The double mutants fed with NPD were hypophosphatemic by 6 wk of age (7.3±0.2 mg/dl) compared with wild-type mice (8.5±0.6 mg/dl) of similar age. The high serum phosphate levels in *NaPi2a*$^{-/-}$/*klotho*$^{-/-}$ mice fed with HPD (11.8±0.6 mg/dl) were similar to those seen in age-matched *klotho*$^{-/-}$ mice (12.1±0.6 mg/dl) at 6 wk of age but different from those of *NaPi2a*$^{-/-}$/*klotho*$^{-/-}$ mice fed with NPD. Similar patterns of serum phosphate levels were also observed in 9-wk-old mice (**Fig. 2**). Collectively, these findings suggest that inactivating NaPi2a function in *klotho* mice reverts hyperphosphatemia to hypophosphatemia.

We also measured serum calcium levels in the various genotypes. Compared with wild-type mice (7.6±0.4

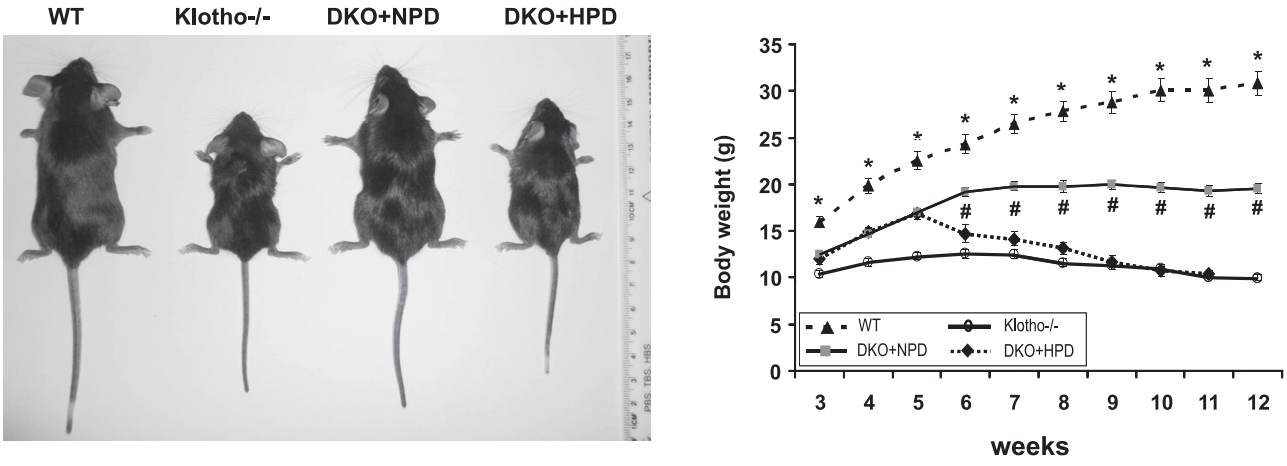

Figure 1. Gross phenotypes of mice. Gross features of wild-type (WT) mice, *klotho*$^{-/-}$ mice, *NaPi2a*$^{-/-}$/*klotho*$^{-/-}$ mice fed with a normal-phosphate diet (DKO+NPD), and *NaPi2a*$^{-/-}$/*klotho*$^{-/-}$ mice fed with a high-phosphate diet (DKO+HPD) at ~9 wk of age (left panel). Body weight curves (right panel) for the 4 different categories show that DKO+HPD mice (n=7) are significantly smaller than DKO+NPD mice (n=46). When compared with WT mice (n=22), hyperphosphatemic *klotho*$^{-/-}$ mice (n=23) are significantly smaller. Note that DKO+NPD mice are larger than *klotho*$^{-/-}$ mice, suggesting that reducing serum phosphate levels in *klotho*$^{-/-}$ mice can help to increase body weight in DKO+NPD mice. *$P < 0.0001$, WT *vs.* *klotho*$^{-/-}$ mice; $^{\#}P < 0.001$, DKO+NPD *vs.* DKO+HPD.

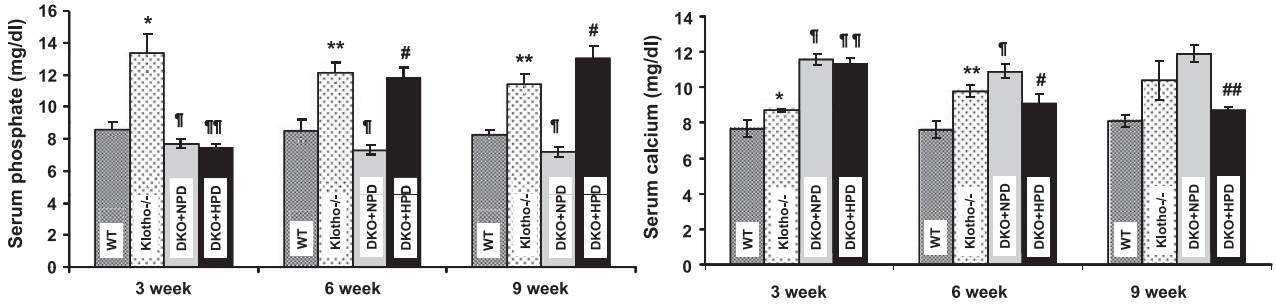

Figure 2. Serum phosphate and calcium levels. Serum phosphate and calcium levels in WT, *klotho*$^{-/-}$, DKO+NPD, and DKO+HPD mice at 3, 6, and 9 wk of age. Serum phosphate (left panel) and calcium (right panel) levels are higher in *klotho*$^{-/-}$ mice when compared with WT mice at 3, 6, and 9 wk of age. In contrast to *klotho*$^{-/-}$ mice, serum phosphate levels are markedly reduced in DKO+NPD mice. Serum phosphate levels are significantly increased in DKO+HPD mice. Increased serum calcium levels are observed in normal-phosphate diet-fed *klotho*$^{-/-}$ and DKO+NPD mice compared with WT controls, but levels are slightly lower in DKO+HPD mice. $^{*}P < 0.05$, $^{**}P < 0.01$ *vs.* WT; $^{¶}P < 0.01$, $^{¶¶}P < 0.001$ *vs. klotho*$^{-/-}$; $^{\#}P < 0.05$, $^{\#\#}P < 0.001$ *vs.* DKO+NPD.

mg/dl at 6 wk), *klotho*$^{-/-}$ mice showed elevated serum calcium levels (9.8±0.3 mg/dl at 6 wk) at all measured time points, and a similar pattern was also noted in *NaPi2a*$^{-/-}$/*klotho*$^{-/-}$ mice fed either with NPD (10.9±0.4 mg/dl at 6 wk) or HPD (9.1±0.5 mg/dl at 6 wk; Fig. 2). Serum calcium levels in NPD-fed *NaPi2a*$^{-/-}$/*klotho*$^{-/-}$ mice, however, were slightly higher than in HPD-fed *NaPi2a*$^{-/-}$/*klotho*$^{-/-}$ mice.

Phosphate toxicity and premature aging-like phenotypes

In contrast to the normal phenotype of heterozygous *klotho*-mutant mice, homozygous *klotho* mutants displayed numerous features resembling premature aging from 3 wk onwards, including visible growth retardation, sluggish movement, infertility, and premature death between 7 and 15 wk. Hyperphosphatemic *klotho*$^{-/-}$ mice were easily recognized by their small size and marked kyphosis. The genital organs in both sexes of *klotho*$^{-/-}$ mice were severely atrophic as observed by macroscopic and microscopic examinations (Supplemental Fig. 2); this severe hypogonadism in both sexes results in infertility, which is a major consequence of aging in both humans and experimental animals (6, 31). The crossbreeding between homozygous *klotho* mice or between double-homozygous *NaPi2a*/*klotho* mice fed with HPD did not produce any offspring, despite an extended period of mating. Interestingly, when serum phosphate levels were reduced for *klotho*$^{-/-}$ mice, the *NaPi2a*$^{-/-}$/*klotho*$^{-/-}$ double-mutant mice fed with NPD recovered body weight, regained fertility, and most important, survived longer. Neither *NaPi2a*$^{-/-}$/*klotho*$^{-/-}$ mice fed with HPD nor *klotho*$^{-/-}$ mice survived past 15 wk, while all wild-type mice and *NaPi2a*$^{-/-}$/*klotho*$^{-/-}$ mice fed with NPD survived beyond 20 wk (**Fig. 3**). The rescue of premature aging-like phenotypes of *NaPi2a*$^{-/-}$/*klotho*$^{-/-}$ mice fed with NPD can be reversed by feeding *NaPi2a*$^{-/-}$/*klotho*$^{-/-}$ double-mutant mice with HPD, clearly suggesting that phosphate toxicity is driving the premature aging-like features in *klotho*-mutant mice.

Effects of phosphate toxicity on lung, intestine, and skin

Hyperphosphatemic *klotho*$^{-/-}$ mice showed typical features of emphysema in the lungs (**Fig. 4**), which appeared as early as 6 wk of age and are consistent with similar emphysematous changes documented in aged populations (32). Reducing serum phosphate levels in *klotho*$^{-/-}$ mice suppressed emphysematous changes in the *NaPi2a*$^{-/-}$/*klotho*$^{-/-}$ double-mutant mice. However, feeding *NaPi2a*$^{-/-}$/*klotho*$^{-/-}$ double mutants with HPD induced severe emphysema, clearly suggesting a role for phosphate toxicity in this lung pathology.

Reduction in villus height of the intestinal mucosa and reduced mucosal surface area are pathologies usually noted in aged populations (33). Compared with wild-type mice, *klotho*$^{-/-}$ mice showed focal areas of intestinal mucosal atrophy with thin muscular layers

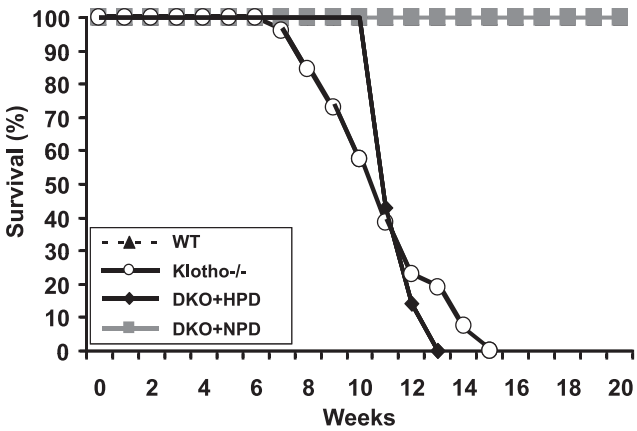

Figure 3. Survival curve. Survival curves for WT (n=17), *klotho*$^{-/-}$ (n=23), DKO+NPD (n=15), and DKO+HPD mice (n=7). Note that the survival of DKO+HPD mice is much lower than for DKO+NPD mice and is similar to hyperphosphatemic *klotho*$^{-/-}$ mice. Most DKO+HPD mice and *klotho*$^{-/-}$ mice die by 15 wk of age, while no WT and DKO+NPD mice had died by the end of the 20-wk observation period.

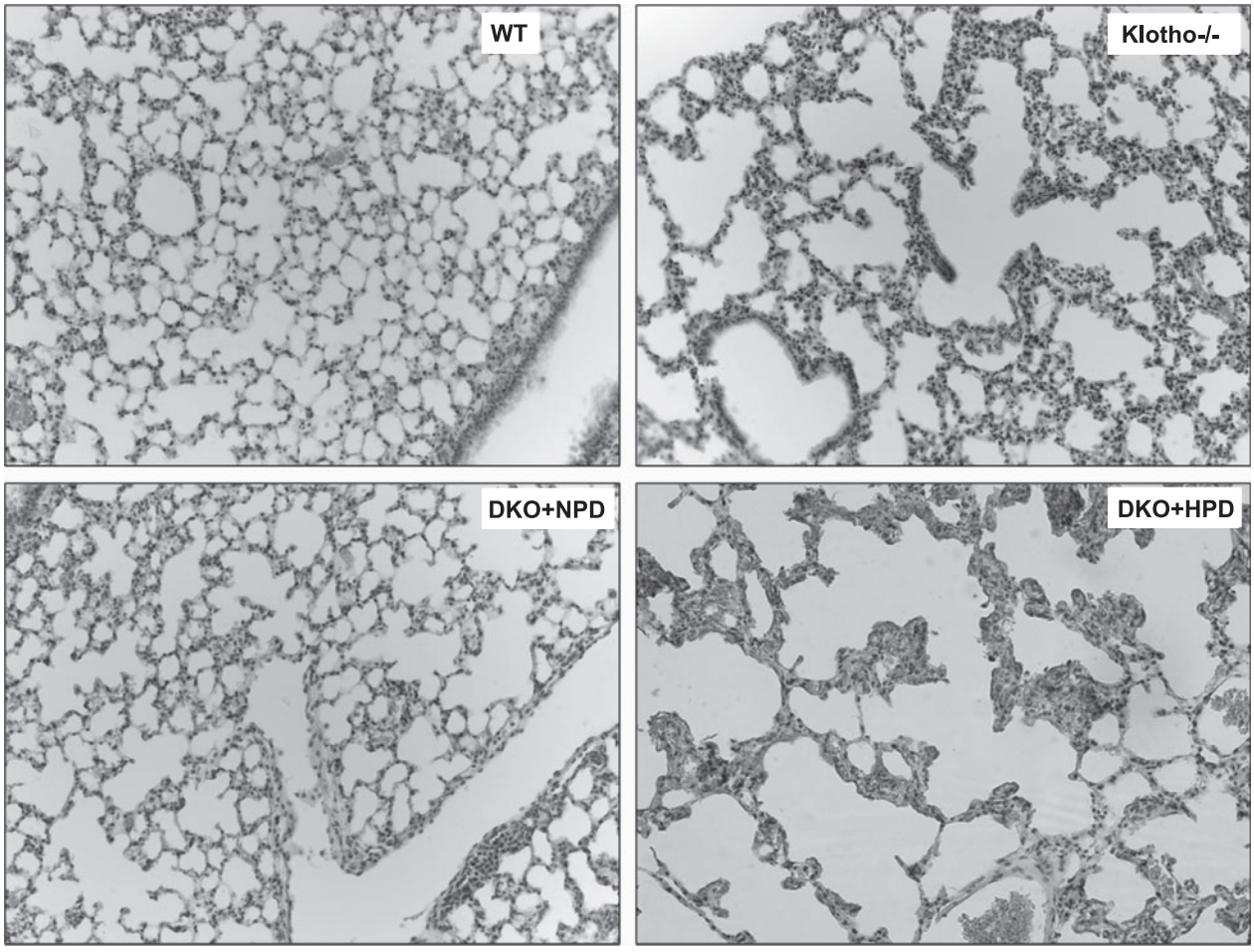

Figure 4. Histological features of lung tissue. Hematoxylin and eosin-stained sections of lungs from 9- to 11-wk-old WT, *klotho*$^{-/-}$, DKO+NPD, and DKO+HPD mice. Compared with WT mice, there is marked expansion of alveolar spaces (emphysema) in *klotho*$^{-/-}$ mice. Such pulmonary emphysematous changes are reduced in DKO+NPD mice and reappear in DKO+HPD. Lungs are fixed in formalin for at least 24 h and then processed in the paraffin before sectioning and staining (view ×10).

(**Fig. 5**). Such intestinal lesions are reduced in hypophosphatemic *NaPi2a*$^{-/-}$/*klotho*$^{-/-}$ double-mutant mice (fed with NPD) and reappear in hyperphosphatemic *NaPi2a*$^{-/-}$/*klotho*$^{-/-}$ double mutants (fed with HPD), implicating a pathological role for phosphate toxicity in intestinal atrophy.

Hairs are sparser in the skin of the *klotho*$^{-/-}$ mice than in control littermates. A reduced number of hair follicles with markedly reduced dermal and epidermal thickness as well as barely detectable subcutaneous fat were consistently noted in hyperphosphatemic *klotho*$^{-/-}$ mice (**Fig. 6**). When serum phosphate levels were reduced in *klotho*$^{-/-}$ mice, there were obvious improvements in skin structure in the *NaPi2a*$^{-/-}$/*klotho*$^{-/-}$ double mutants, with clearly apparent subcutaneous fat layers. The rescue of skin phenotypes for hypophosphatemic *NaPi2a*$^{-/-}$/*klotho*$^{-/-}$ mice (fed with NPD) was reversed in hyperphosphatemic *NaPi2a*$^{-/-}$/*klotho*$^{-/-}$ double-mutant mice (fed with HPD). The abnormal changes in lung (Fig. 4), intestine (Fig. 5), and skin (Fig. 6) for hyperphosphatemic *klotho*$^{-/-}$ mice were dramatically ameliorated and rescued by genetically lowering serum phosphate levels in hypophosphatemic *NaPi2a*$^{-/-}$/*klotho*$^{-/-}$ double mutants, suggesting a pathological role for phosphate toxicity in soft tissue injury (**Table 1**). In addition, severe atrophy of the thymus and spleen (Supplemental Fig. 3) was noted in hyperphosphatemic *klotho*$^{-/-}$ mice when compared with controls. Again, such atrophy of the thymus and spleen was suppressed in hypophosphatemic *NaPi2a*$^{-/-}$/*klotho*$^{-/-}$ mice (fed with NPD) and reappeared in hyperphosphatemic *NaPi2a*$^{-/-}$/*klotho*$^{-/-}$ double mutants (fed with HPD).

Phosphate toxicity and ectopic calcification

We examined calcification in the various murine genotypes by von Kossa staining. Consistent with our earlier observations, we detected extensive vascular and soft tissue calcification in the aorta, lung (Supplemental Fig. 4), kidney (**Fig. 7**), and other organs in *klotho*$^{-/-}$ mice. The extensive calcification noted in *klotho*$^{-/-}$ mice was absent in *NaPi2a*$^{-/-}$/*klotho*$^{-/-}$ mice fed with NPD but reappeared in *NaPi2a*$^{-/-}$/*klotho*$^{-/-}$ mice fed with HPD, suggesting a crucial role for phosphate in vascular and soft tissue calcification.

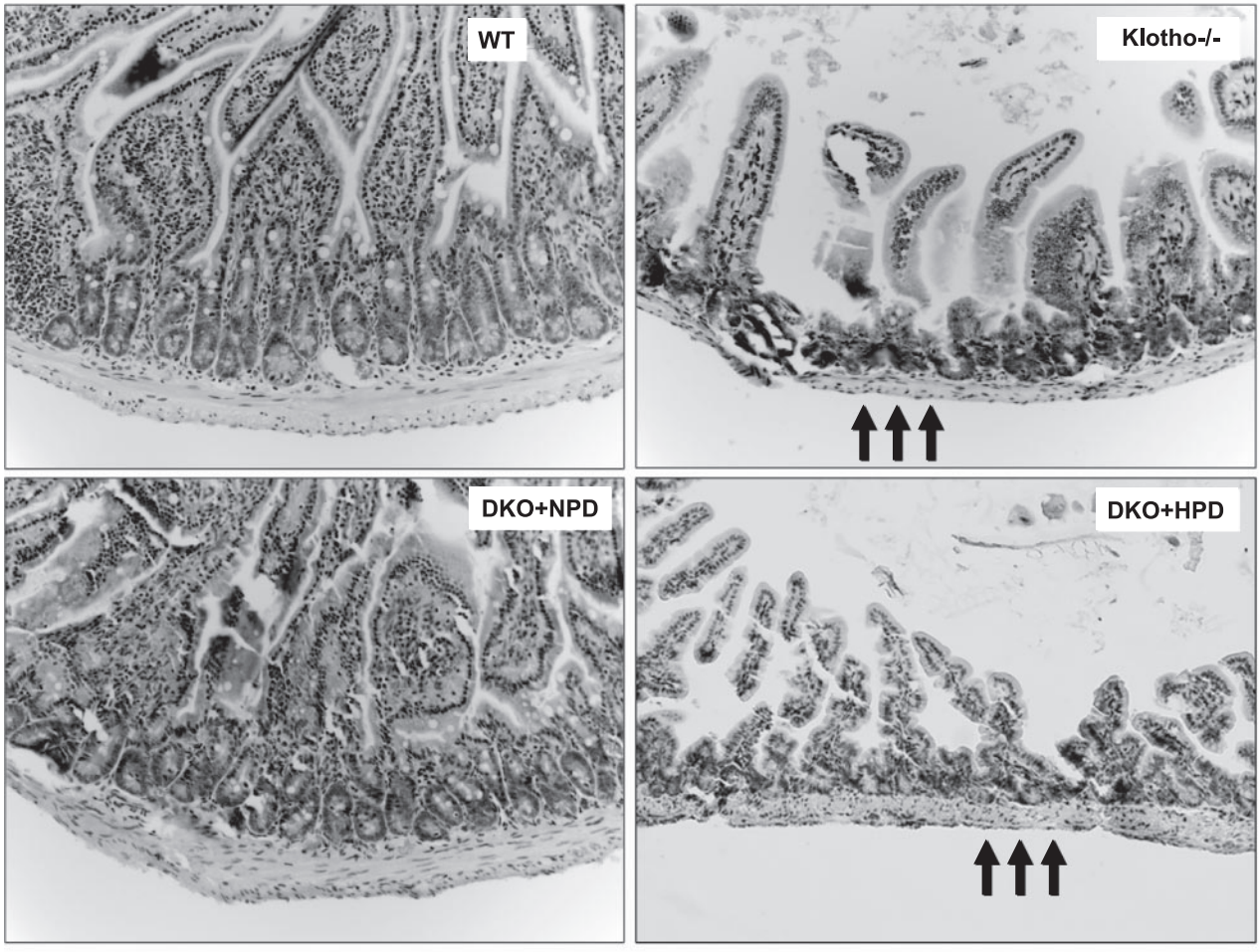

Figure 5. Histological features of intestine. Hematoxylin and eosin-stained sections of intestines from WT, *klotho*$^{-/-}$, DKO+NPD, and DKO+HPD mice. Compared with WT mice, there is marked atrophy of the intestinal wall (arrows) in *klotho*$^{-/-}$ mice. These focal atrophic changes of the intestine are improved in DKO+NPD mice and reappear in DKO+HPD mice, suggesting that reducing serum phosphate levels in the *klotho*$^{-/-}$ mice can help to restore intestinal anomalies (intestine view ×20).

Phosphate toxicity and apoptosis

To elucidate how phosphate toxicity induces generalized tissue anomalies, we used TUNEL staining to determine the numbers of apoptotic cells in various tissues obtained from wild-type, *klotho*$^{-/-}$, and *NaPi2a*$^{-/-}$/*klotho*$^{-/-}$ mice fed with either NPD or HPD. There is an increase in the number of apoptotic cells in kidneys from hyperphosphatemic *klotho*$^{-/-}$ mice (**Fig. 8**). The number of apoptotic cells was significantly reduced in hypophosphatemic *NaPi2a*$^{-/-}$/*klotho*$^{-/-}$ double mutants (fed with NPD) and markedly increased in hyperphosphatemic *NaPi2a*$^{-/-}$/*klotho*$^{-/-}$ double mutants (fed with HPD). Similar pattern of apoptosis is also noted in lung and skeletal muscle. Impairment of cellular homeostasis following an increased rate of apoptosis caused by phosphate toxicity may contribute to generalized tissue anomalies.

DISCUSSION

We present here a novel role for phosphate in accelerating the mammalian aging process and reducing survival. Our results show that genetically ablated *klotho* mice develop extensive premature aging-like features, which include but are not limited to loss of body weight, kyphosis, hypogonadism, infertility, generalized tissue atrophy, and reduced life span. These all bear similarity to phenotypes observed during human aging. Despite the fact that expression of the *klotho* gene is very restricted and is mainly found in the kidney, parathyroid gland, and pituitary gland (34, 35), *klotho*-knockout mice show systemic premature aging-like phenotypes (20, 21, 36). Generalized involvement of tissues and organs outside *klotho*-expressing tissues in knockout mice suggests that these premature aging-like features are likely to be non-cell autonomous. It is possible that dysregulation of the physiological balance caused by loss of *klotho* function induces systemic aging-like features. In fact, the extensive age-associated phenotypes in *klotho*-knockout mice can be suppressed by genetically reducing serum phosphate levels in *NaPi2a*$^{-/-}$/*klotho*$^{-/-}$ DKO mice, thus extending survival. More important, when serum phosphate levels are increased in *NaPi2a*$^{-/-}$/*klotho*$^{-/-}$ DKO mice by

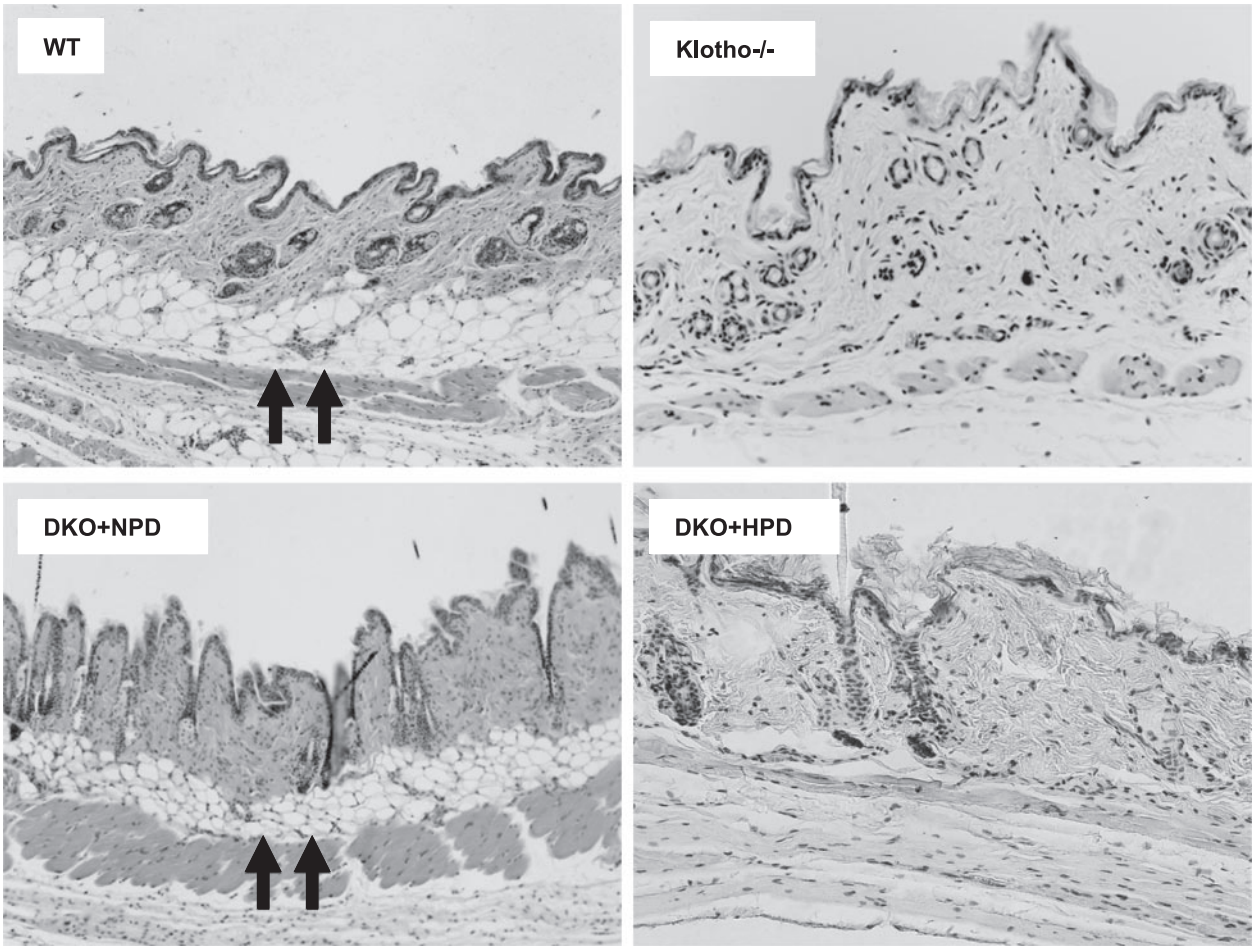

Figure 6. Histological features of skin tissues. Hematoxylin and eosin-stained sections of skin from 9- to 11-wk-old WT, *klotho*$^{-/-}$, DKO+NPD, and DKO+HPD mice. Compared with WT mice, there is marked atrophy of the skin in *klotho*$^{-/-}$ mice. Subcutaneous fat tissue layer (arrows) seen in wild-type skin is mostly absent in *klotho* homozygous mutant mice. Such focal atrophic changes are improved in DKO+NPD mice and reappear in DKO+HPD mice, suggesting a role for phosphate toxicity in skin atrophy (view ×10 for WT and DKO+NPD; ×20 for *klotho*$^{-/-}$ and DKO+HPD).

feeding with an HPD, the premature aging-like features reappear in the DKO mice similarly as in *klotho* single mutants. These results clearly suggest that phosphate toxicity is the main cause of premature aging-like features in *klotho* knockouts. Of relevance, compared with the wild-type controls, the serum 1,25-dehydroxyvitamin D levels were higher in *klotho*$^{-/-}$ mice and in *NaPi2a*$^{-/-}$/*klotho*$^{-/-}$ mice fed either with an HPD or NPD (Supplemental Fig. 5); these results suggest that rescue of premature aging-like features in *NaPi2a*$^{-/-}$/*klotho*$^{-/-}$ mice fed with an NPD and reappearance in *NaPi2a*$^{-/-}$/*klotho*$^{-/-}$ mice fed with an HPD are independent of vitamin D activities. Moreover, the rescue of premature aging-like features of *klotho*$^{-/-}$mice by inactivating vitamin D activities (in *1a-hydroxylase*$^{-/-}$/*klotho*$^{-/-}$ DKO mice) is due to reduced serum phosphate levels in double-mutant mice (37). A similar pattern of rescue is also noted in fibroblast growth factor 23 (Fgf23)-knockout mice without vitamin D activity (in *1a-hydroxylase*$^{-/-}$/*Fgf23*$^{-/-}$ DKO mice), as we reported in our earlier publications (29, 36, 38).

Klotho mutants show severe hyperphosphatemia leading to widespread tissue atrophy in spleen, skeletal muscle, intestine, and skin. Interestingly, reducing serum phosphate levels in *klotho* knockouts by genetic ablation of the *NaPi2a* gene rescues tissue atrophy in *NaPi2a*$^{-/-}$/*klotho*$^{-/-}$ DKO mice. However, feeding *NaPi2a*$^{-/-}$/*klotho*$^{-/-}$ DKO mice with an HPD results in severe tissue atrophy, suggesting that the generalized tissue atrophy in *klotho* mutants is partly caused by phosphate toxicity. The *klotho*-knockout mice have severe muscle wasting with reduced fat tissue. Lowering serum phosphate levels from *klotho*-knockout mice not only reduced muscle wasting but also helped gain fat tissues; whether such improvements in the muscle and the fat tissues result in better survival of *NaPi2a*$^{-/-}$/*klotho*$^{-/-}$ DKO mice will need additional studies.

Consistent with our earlier observations, hyperphosphatemic *klotho*-knockout mice show typical features of emphysema in the lungs, which mostly disappear in the NPD-fed *NaPi2a*$^{-/-}$/*klotho*$^{-/-}$ DKO mice (23). However, emphysema in the lungs reappears in *NaPi2a*$^{-/-}$/*klotho*$^{-/-}$ DKO mice fed with an HPD, implicating phosphate toxicity in lung damage. Of relevance to this observation, emphysematous changes have also been documented in aged populations (32).

TABLE 1. *Phenotypes of various mutant mice compared with those of wild-type mice*

Phenotype	Wild-type (NPD)	*klotho*$^{-/-}$ (NPD)	*klotho*$^{-/-}$/*NaPi2a*$^{-/-}$ (NPD)	*klotho*$^{-/-}$/*NaPi2a*$^{-/-}$ (HPD)
Biochemical changes				
Serum phosphate	Normal	High	Low/normal	High
Serum calcium	Normal	High (M)	High (M)	High (S)
Gross appearance				
Body weight	Normal	Reduced (M)	Reduced (S)	Reduced (M)
Growth retardation	Absent	Present (M)	Present (S)	Present (M)
Kyphosis	Absent	Present	Absent	Present
Generalized atrophy				
Spleen atrophy	Absent	Present	Absent	Present
Muscle atrophy	Absent	Present	Absent	Present
Skin atrophy	Absent	Present	Absent	Present
Intestinal atrophy	Absent	Present	Absent	Present
Gonadal atrophy	Absent	Present	Absent	Present
Morphological changes				
Vascular calcifications	Absent	Present	Absent	Present
Ectopic calcifications	Absent	Present	Absent	Present
Emphysema	Absent	Present (D)	Present (F)	Present (D)
Overall affect				
Physical activity	Normal	Sluggish	Normal	Sluggish
Fertility	Normal	Lost	Normal	Lost
Lifespan	Normal	Short	Normal	Short

Note that the phenotypes of the NPD-fed *klotho*$^{-/-}$ mice and *klotho*$^{-/-}$/*NaPi2a*$^{-/-}$ double-knockout mice are consistent with our earlier reported observations (23). M, markedly; S, slightly; D, diffuse; F, focal.

The genital organs of both sexes of hyperphosphatemic *klotho*-knockout mice are severely atrophic as observed by macroscopic and microscopic examinations; this severe hypogonadism in both sexes results in infertility, which is a major consequence of aging in both humans and experimental animals (6, 31). The *klotho*-knockout mice with reduced serum phosphate levels regained fertility, as evidenced in the *NaPi2a*$^{-/-}$/*klotho*$^{-/-}$ DKO mice. More important, the *NaPi2a*$^{-/-}$/*klotho*$^{-/-}$ DKO mice lost their fertility when fed with an HPD, clearly suggesting that phosphate toxicity can affect fertility and thereby influence the aging process.

The mechanism by which phosphate toxicity accelerates the aging process requires further study. It is likely that high phosphate exerts its cytotoxic effects to compromise the physiological functions of various organ systems. We found that high phosphate can induce an increased rate of apoptosis in various organs and that this apoptosis is suppressed by lowering serum phosphate levels in the *NaPi2a*$^{-/-}$/*klotho*$^{-/-}$ DKO mice. It is likely that continued cell deletion through apoptosis and due to phosphate toxicity leads to generalized tissue atrophy as well as reduced organ function and viability, thereby accelerating the aging-like

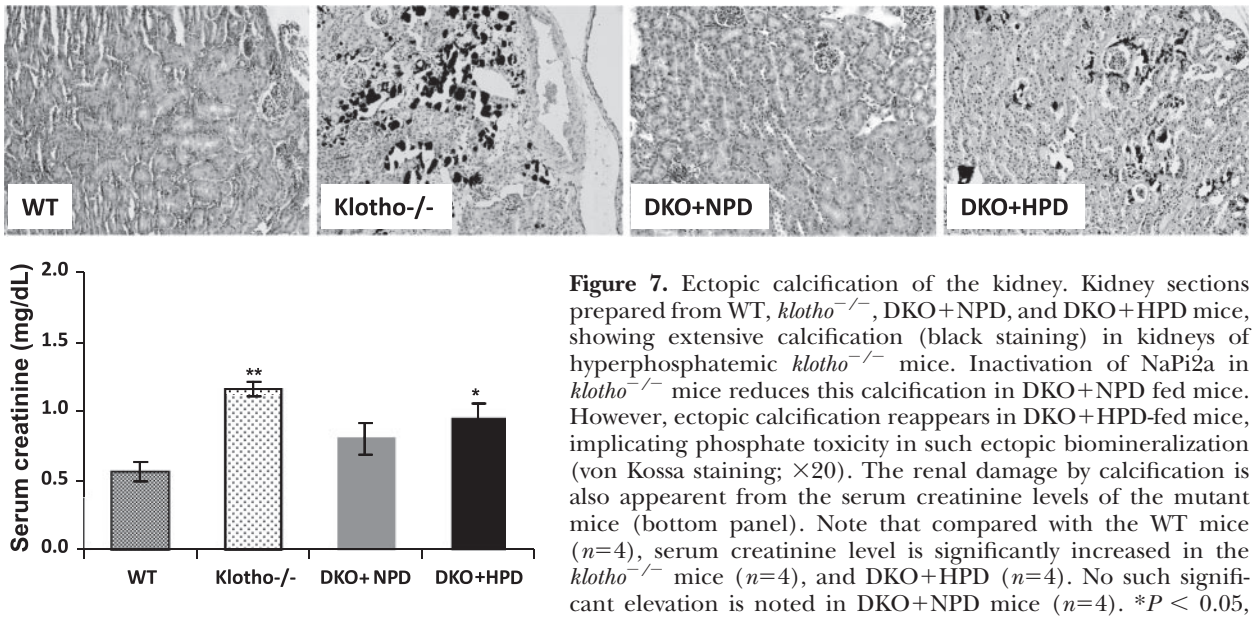

Figure 7. Ectopic calcification of the kidney. Kidney sections prepared from WT, *klotho*$^{-/-}$, DKO+NPD, and DKO+HPD mice, showing extensive calcification (black staining) in kidneys of hyperphosphatemic *klotho*$^{-/-}$ mice. Inactivation of NaPi2a in *klotho*$^{-/-}$ mice reduces this calcification in DKO+NPD fed mice. However, ectopic calcification reappears in DKO+HPD-fed mice, implicating phosphate toxicity in such ectopic biomineralization (von Kossa staining; ×20). The renal damage by calcification is also appearent from the serum creatinine levels of the mutant mice (bottom panel). Note that compared with the WT mice (n=4), serum creatinine level is significantly increased in the *klotho*$^{-/-}$ mice (n=4), and DKO+HPD (n=4). No such significant elevation is noted in DKO+NPD mice (n=4). *$P < 0.05$, **$P < 0.01$ *vs.* WT.

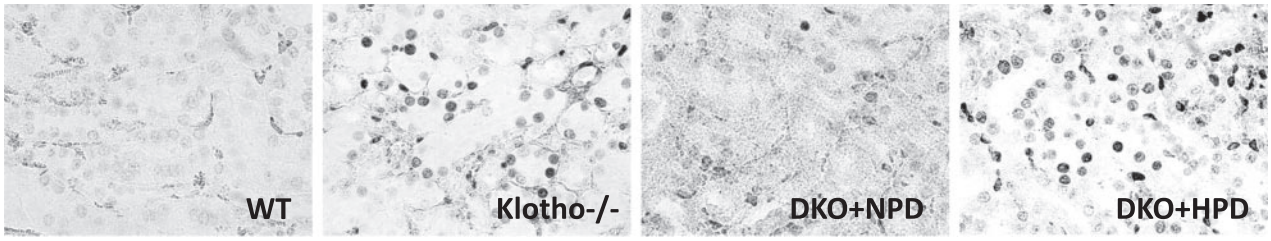

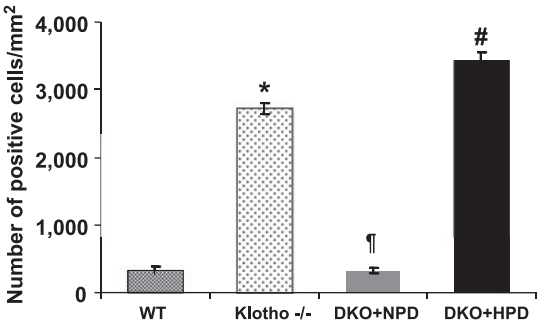

Figure 8. Apoptotic cells in the kidney. Detection of TUNEL-positive cells in kidney sections prepared from WT, *klotho*$^{-/-}$, DKO+NPD, and DKO+HPD mice. Kidney sections prepared from *klotho*$^{-/-}$ and DKO+HPD mice showing increased numbers of apoptotic cells when compared with kidneys of WT and DKO+NPD mice. Note that, compared with the hyperphosphatemic *klotho*$^{-/-}$ mice, the hypophosphatemic *NaPi2a*$^{-/-}$/*klotho*$^{-/-}$ mice (fed with NPD) have reduced apoptotic cell death, while inducing hyperphosphatemia in *NaPi2a*$^{-/-}$/*klotho*$^{-/-}$ double mutants (fed with HPD) increases apoptotic cell death, which is similar to *klotho*$^{-/-}$ mice (view ×60). *$P < 0.001$ *vs.* WT; ¶$P < 0.001$ *vs.* *klotho*$^{-/-}$; #$P < 0.001$ *vs.* DKO+NPD.

process as noted in our mouse models. In a similar line of observation, extensive renal calcification with increased numbers of apoptotic cells in the kidneys of the hyperphosphatemic mutant mice is associated with increased serum levels of creatinine (Fig. 7); such impairment of renal function may contribute to the reduced survival of *klotho*-knockout mice and *NaPi2a*$^{-/-}$/*klotho*$^{-/-}$ mice fed with an HPD (26, 39).

CONCLUSIONS

The results of our *in vivo* genetic and dietary manipulation studies provide evidence for a novel role of phosphate in mammalian aging. Our results showing that genetically reducing serum phosphate levels in *klotho*-knockout mice suppresses the aging-like phenotypes in *NaPi2a*$^{-/-}$/*klotho*$^{-/-}$ DKO mice and that increasing serum phosphate levels in *NaPi2a*$^{-/-}$/*klotho*$^{-/-}$ DKO mice accelerates the aging-like phenotype to reduce longevity support a role for phosphate toxicity in regulating the aging process. One of the limitations of the generated *NaPi2a*$^{-/-}$/*klotho*$^{-/-}$ DKO mice is that loss of NaPi2a function can be gradually compensated by other phosphate transporters, including NaPi2c, which is particularly apparent in the aged DKO mice. Aged *NaPi2a*$^{-/-}$/*klotho*$^{-/-}$ DKO mice have relatively higher serum phosphate levels and that may influence survival of these mice, again suggesting a role of phosphate in aging and survival. Finally, *NaPi2a*$^{-/-}$/*klotho*$^{-/-}$ DKO mice provide an important *in vivo* tool to study the effects of various dietary components on aging. Our understanding of intrinsic factors that accelerate aging may provide better insights into the mechanisms by which extrinsic factors influence mammalian senescence. FJ

Parts of this research were supported by National Institute of Diabetes and Digestive and Kidney Disease grant R01-DK-077276 (to M.S.R.).

REFERENCES

1. Dolle, M. E., Giese, H., Hopkins, C. L., Martus, H. J., Hausdorff, J. M., and Vijg, J. (1997) Rapid accumulation of genome rearrangements in liver but not in brain of old mice. *Nat. Genet.* **17,** 431–434
2. Kirkwood, T. B., and Austad, S. N. (2000) Why do we age? *Nature* **408,** 233–238
3. De Boer, J., Andressoo, J. O., de Wit, J., Huijmans, J., Beems, R. B., van Steeg, H., Weeda, G., van der Horst, G. T., van Leeuwen, W., Themmen, A. P., Meradji, M., and Hoeijmakers, J. H. (2002) Premature aging in mice deficient in DNA repair and transcription. *Science* **296,** 1276–1279
4. Tarry-Adkins, J. L., Chen, J. H., Smith, N. S., Jones, R. H., Cherif, H., and Ozanne, S. E. (2009) Poor maternal nutrition followed by accelerated postnatal growth leads to telomere shortening and increased markers of cell senescence in rat islets. *FASEB J.* **23,** 1521–1528
5. Kujoth, G. C., Hiona, A., Pugh, T. D., Someya, S., Panzer, K., Wohlgemuth, S. E., Hofer, T., Seo, A. Y., Sullivan, R., Jobling, W. A., Morrow, J. D., Van Remmen, H., Sedivy, J. M., Yamasoba, T., Tanokura, M., Weindruch, R., Leeuwenburgh, C., and Prolla, T. A. (2005) Mitochondrial DNA mutations, oxidative stress, and apoptosis in mammalian aging. *Science* **309,** 481–484
6. Trifunovic, A., Wredenberg, A., Falkenberg, M., Spelbrink, J. N., Rovio, A. T., Bruder, C. E., Bohlooly, Y. M., Gidlof, S., Oldfors, A., Wibom, R., Tornell, J., Jacobs, H. T., and Larsson, N. G. (2004) Premature ageing in mice expressing defective mitochondrial DNA polymerase. *Nature* **429,** 417–423
7. Jang, Y. C., Lustgarten, M. S., Liu, Y., Muller, F. L., Bhattacharya, A., Liang, H., Salmon, A. B., Brooks, S. V., Larkin, L., Hayworth, C. R., Richardson, A., and Van Remmen, H. (2009) Increased superoxide in vivo accelerates age-associated muscle atrophy through mitochondrial dysfunction and neuromuscular junction degeneration. [E-pub ahead of print] *FASEB J.* doi: 10.1096/fj.09-146308
8. Salmon, A. B., Perez, V. I., Bokov, A., Jernigan, A., Kim, G., Zhao, H., Levine, R. L., and Richardson, A. (2009) Lack of methionine sulfoxide reductase A in mice increases sensitivity to oxidative stress but does not diminish life span. *FASEB J.* **23,** 3601–3608
9. Edwards, M. G., Sarkar, D., Klopp, R., Morrow, J. D., Weindruch, R., and Prolla, T. A. (2003) Age-related impairment of the transcriptional responses to oxidative stress in the mouse heart. *Physiol. Genomics* **13,** 119–127
10. Radak, Z., Chung, H. Y., Naito, H., Takahashi, R., Jung, K. J., Kim, H. J., and Goto, S. (2004) Age-associated increase in oxidative stress and nuclear factor kappaB activation are attenuated in rat liver by regular exercise. *FASEB J.* **18,** 749–750

11. Judge, S., Jang, Y. M., Smith, A., Hagen, T., and Leeuwenburgh, C. (2005) Age-associated increases in oxidative stress and antioxidant enzyme activities in cardiac interfibrillar mitochondria: implications for the mitochondrial theory of aging. *FASEB J.* **19,** 419–421
12. Gaasbeek, A., and Meinders, A. E. (2005) Hypophosphatemia: an update on its etiology and treatment. *Am. J. Med.* **118,** 1094–1101
13. Razzaque, M. S. (2009) FGF23-mediated regulation of systemic phosphate homeostasis: is Klotho an essential player? *Am. J. Physiol. Renal Physiol.* **296,** F470–476
14. Razzaque, M. S. (2009) The FGF23-Klotho axis: endocrine regulation of phosphate homeostasis. *Nat. Rev. Endocrinol.* **5,** 611–619
15. Razzaque, M. S., and Lanske, B. (2007) The emerging role of the fibroblast growth factor-23-klotho axis in renal regulation of phosphate homeostasis. *J. Endocrinol.* **194,** 1–10
16. Tenenhouse, H. S. (2005) Regulation of phosphorus homeostasis by the type iia na/phosphate cotransporter. *Annu. Rev. Nutr.* **25,** 197–214
17. Nakatani, T., Bara, S., Ohnishi, M., Densmore, M. J., Taguchi, T., Goetz, R., Mohammadi, M., Lanske, B., and Razzaque, M. S. (2009) In vivo genetic evidence of klotho-dependent functions of FGF23 in regulation of systemic phosphate homeostasis. *FASEB J.* **23,** 433–441
18. Segawa, H., Yamanaka, S., Ohno, Y., Onitsuka, A., Shiozawa, K., Aranami, F., Furutani, J., Tomoe, Y., Ito, M., Kuwahata, M., Imura, A., Nabeshima, Y., and Miyamoto, K. (2007) Correlation between hyperphosphatemia and type II Na-Pi cotransporter activity in klotho mice. *Am. J. Physiol. Renal Physiol.* **292,** F769–F779
19. Nakatani, T., Ohnishi, M., and Razzaque, M. S. (2009) Inactivation of klotho function induces hyperphosphatemia even in presence of high serum fibroblast growth factor 23 levels in a genetically engineered hypophosphatemic (Hyp) mouse model. *FASEB J.* **23,** 3702–3711
20. Lanske, B., and Razzaque, M. S. (2007) Premature aging in klotho mutant mice: cause or consequence? *Ageing Res. Rev.* **6,** 73–79
21. Kuro-o, M., Matsumura, Y., Aizawa, H., Kawaguchi, H., Suga, T., Utsugi, T., Ohyama, Y., Kurabayashi, M., Kaname, T., Kume, E., Iwasaki, H., Iida, A., Shiraki-Iida, T., Nishikawa, S., Nagai, R., and Nabeshima, Y. I. (1997) Mutation of the mouse klotho gene leads to a syndrome resembling ageing. *Nature* **390,** 45–51
22. Beck, L., Karaplis, A. C., Amizuka, N., Hewson, A. S., Ozawa, H., and Tenenhouse, H. S. (1998) Targeted inactivation of Npt2 in mice leads to severe renal phosphate wasting, hypercalciuria, and skeletal abnormalities. *Proc. Natl. Acad. Sci. U. S. A.* **95,** 5372–5377
23. Ohnishi, M., Nakatani, T., Lanske, B., and Razzaque, M. S. (2009) In vivo genetic evidence for suppressing vascular and soft-tissue calcification through the reduction of serum phosphate levels, even in the presence of high serum calcium and 1,25-Dihydroxyvitamin D levels. *Circ. Cardiovasc. Genet.* **2,** 583–590
24. Sitara, D., Kim, S., Razzaque, M. S., Bergwitz, C., Taguchi, T., Schuler, C., Erben, R. G., and Lanske, B. (2008) Genetic evidence of serum phosphate-independent functions of FGF-23 on bone. *PLoS Genet.* **4,** e1000154
25. Razzaque, M. S., Kumatori, A., Harada, T., and Taguchi, T. (1998) Coexpression of collagens and collagen-binding heat shock protein 47 in human diabetic nephropathy and IgA nephropathy. *Nephron* **80,** 434–443
26. Zha, Y., Le, V. T., Higami, Y., Shimokawa, I., Taguchi, T., and Razzaque, M. S. (2006) Life-long suppression of growth hormone-insulin-like growth factor I activity in genetically altered rats could prevent age-related renal damage. *Endocrinology* **147,** 5690–5698
27. Razzaque, M. S., Soegiarto, D. W., Chang, D., Long, F., and Lanske, B. (2005) Conditional deletion of Indian hedgehog from collagen type 2alpha1-expressing cells results in abnormal endochondral bone formation. *J. Pathol.* **207,** 453–461
28. Razzaque, M. S., and Taguchi, T. (1997) Collagen-binding heat shock protein (HSP) 47 expression in anti-thymocyte serum (ATS)-induced glomerulonephritis. *J. Pathol.* **183,** 24–29
29. Razzaque, M. S., Sitara, D., Taguchi, T., St-Arnaud, R., and Lanske, B. (2006) Premature aging-like phenotype in fibroblast growth factor 23 null mice is a vitamin-D mediated process. *FASEB J.* **20,** 720–722
30. Razzaque, M. S., Koji, T., Kumatori, A., and Taguchi, T. (1999) Cisplatin-induced apoptosis in human proximal tubular epithelial cells is associated with the activation of the Fas/Fas ligand system. *Histochem. Cell Biol.* **111,** 359–365
31. Rauser, C. L., Mueller, L. D., and Rose, M. R. (2003) Aging, fertility, and immortality. *Exp. Gerontol.* **38,** 27–33
32. Martin, C. J., Chihara, S., and Chang, D. B. (1977) A comparative study of the mechanical properties in aging alveolar wall. *Am. Rev. Respir. Dis.* **115,** 981–988
33. Evers, B. M., Townsend, C. M., Jr., and Thompson, J. C. (1994) Organ physiology of aging. *Surg. Clin. North Am.* **74,** 23–39
34. Kato, Y., Arakawa, E., Kinoshita, S., Shirai, A., Furuya, A., Yamano, K., Nakamura, K., Iida, A., Anazawa, H., Koh, N., Iwano, A., Imura, A., Fujimori, T., Kuro-o, M., Hanai, N., Takeshige, K., and Nabeshima, Y. (2000) Establishment of the anti-Klotho monoclonal antibodies and detection of Klotho protein in kidneys. *Biochem. Biophys. Res. Commun.* **267,** 597–602
35. Li, S. A., Watanabe, M., Yamada, H., Nagai, A., Kinuta, M., and Takei, K. (2004) Immunohistochemical localization of Klotho protein in brain, kidney, and reproductive organs of mice. *Cell Struct. Funct.* **29,** 91–99
36. Razzaque, M. S., and Lanske, B. (2006) Hypervitaminosis D and premature aging: lessons learned from Fgf23 and Klotho mutant mice. *Trends Mol. Med.* **12,** 298–305
37. Ohnishi, M., Nakatani, T., Lanske, B., and Razzaque, M. S. (2009) Reversal of mineral ion homeostasis and soft-tissue calcification of klotho knockout mice by deletion of vitamin D 1alpha-hydroxylase. *Kidney Int.* **75,** 1166–1172
38. Razzaque, M. S., St-Arnaud, R., Taguchi, T., and Lanske, B. (2005) FGF-23, vitamin D and calcification: the unholy triad. *Nephrol. Dial. Transplant.* **20,** 2032–2035
39. Razzaque, M. S. (2007) Does renal ageing affect survival? *Ageing Res. Rev.* **6,** 211–222

Received for publication March 8, 2010.
Accepted for publication April 9, 2010.